Recognition of Power Quality Disturbances in Renewable Energy Sources Based Smart Grid Using Stockwell Transform

Yogesh Mehta [1], Ravindra Prakash Gupta [2] and O. S. Lamba [1]

[1] Department of Electronics and Communications Engineering, Gyan Vihar University, Jaipur, India

[2] Department of Electronics and Communications Engineering, Manda Institute of Tech., Bikaner, India

Abstract

This paper presents an approach for the detection of power quality disturbances in smart grid associated with the events such as feeder tripping/reclosing, switching on/off of the capacitor banks and switching on/off the inductive-resistive (RL) loads. The distributed generation (DG) sources are integrated to the smart grid. The proposed study has been carried out using a standard IEEE-13 bus distribution network modelled as smart grid incorporated with wind and solar PV systems. The proposed test system is simulated using MATLAB software in simulink environment. Voltage signals captured at the point of common coupling (PCC) of the test system are decomposed using Stockwell's transform for power quality analysis. The harmonic detection has been carried out using Fast Fourier Transform. The power quality disturbances associated with the events under study have been investigated using the Stockwell transform based plots.

Keywords: *Power quality, solar PV system, smart grid, Stockwell's transform, wind energy conversion system*

1. Introduction

Recently the quality of electrical power is taken care by both the utilities and consumers. Power quality (PQ) is defined as the deviation in the current, voltage and frequency from their values specified by the standards. The poor power quality include the disturbances such as voltage sag, swell, impulsive transient (IT), oscillatory transient (OT), harmonics, multiple notches, spikes, voltage flicker, momentary interruption (MI) etc. [1]. Poor power quality might results in the misoperation or failure of the customer equipments as well as the power system equipments. The integration of distributed energy (DG) sources such as solar photovoltaic (PV) system, wind energy and fuel cell to the smart grids affects the power quality, degrade system reliability and cause over-voltages in the network [2]. This also affects the operation and communication systems of the smart grids. The power fluctuations at the output of wind and solar PV systems due to type of turbines and solar PV systems, variations in the wind and solar insolation over a period may lead to PQ disturbances like voltage sag and swell along with reactive power flow [3]. The detection and localization of the PQ events associated with outage and grid synchronization of solar PV plant in distribution network are investigated in [4]. PQ events associated with the change in solar insolation has also been investigated. Power quality disturbances associated with the events such as islanding, grid synchronization and outage of wind generators have been investigated in [5]. The operational issues in the DG sources based smart grids may also affect the quality of power supplied. Ultimately, this poor quality of the power affects the operations of the smart grids.

Advanced signal processing as well as the artificial intelligent (AI) techniques have been utilized for the recognition of PQ disturbances in the power system and hybrid power system networks. Various signal processing and mathematical techniques used for the detection and classification of the power quality disturbances are reported in [6]. The Fourier transform (FT) and short time Fourier transform (STFT) are used for detection of PQ disturbances with poor detection and classification efficiency. The continuous wavelet transform (CWT) and its discrete version known as discrete wavelet transform (DWT) decomposes the signal into non-uniform frequency bands based on multi-resolution analysis (MRA). Both the CWT and DWT are successfully utilized for detection of PQ disturbances [7]. Stockwell's transform (S-transform) is an extension of the continuous wavelet transform (CWT) and Fourier transform. It is based on a moving and scalable Gaussian window. Stockwell transform provides a frequency-dependent resolution while maintaining a direct relationship with the FT [8]. The S-transform can detect the PQ disturbances with improved efficiency [9]. An algorithm for the detection and classification of PQ disturbances using a fast variant of S-transform and decision tree based classifier is reported in [10]. A probabilistic PQ index for utility grids with increased penetration level of wind power generations is reported in [11]. A method for detection of islanding and power quality disturbances in distributed generation based hybrid power system is reported in [12]. Hsu *et al*. [13] investigated the impacts of large wind power generation system on the distribution system.

Therefore, based on the above reviews, this paper has considered S-transform for the detection of events such as feeder tripping/reclosing, switching on/off of the capacitor banks and switching on/off the RL loads in the wind and solar PV systems based smart grid. The PQ disturbances associated with grid operations of the loads and distribution/transmission lines in the smart grids in the presence of DG sources have not been explored to a much extent. Main contribution of this paper is the design of an algorithm which detects the PQ disturbances associated with events such as feeder tripping/re-closing, switching on/off the capacitor banks and switching on/off the LR loads in the smart grid incorporating the renewable energy sources.

This paper is organized into five sections. Starting with an introduction in the section 1, the section 2 describes the test system used for study. Section 3 presents the proposed methodology for detection of power quality disturbances. Section 4 presents the simulation results with their discussion. The conclusions are presented in the Section 5.

2. Test System Used For Study

This section describes the test system which has been utilized as smart grid incorporated with renewable energy (RE) sources for the study of PQ disturbances under various operating scenarios. A standard IEEE 13 bus test system is modelled as a smart grid. The original system is a 60 Hz, 5 MVA, operated at two voltage levels of 4.16 kV and 0.48 kV. This has the balanced and unbalanced and any DG sources are not integrated to the original system [14]. The test system is modified to incorporate the wind energy conversion system (WECS) and solar PV system on the bus 680 of test system as illustrated in Fig. 1. Bus 680 is considered as PCC. Doubly fed induction generator based wind energy conversion system (WECS) and solar PV system are connected to the test system through transformers XWG and XSPV respectively. The loading status of proposed test system is provided in Table 1. All the feeders of the proposed test system have the configuration 601 of the original IEEE-13 system. Lengths of line segments used in this study are same as in the original test system. The proposed test system of smart grid is connected to the conventional generator using a substation transformer. The transformer connected between the nodes 633 and 634 is named as XFM. Details of transformers are provided in Table 2. Switch between the nodes 671 and 692 have been realized with the help of three phase circuit breaker.

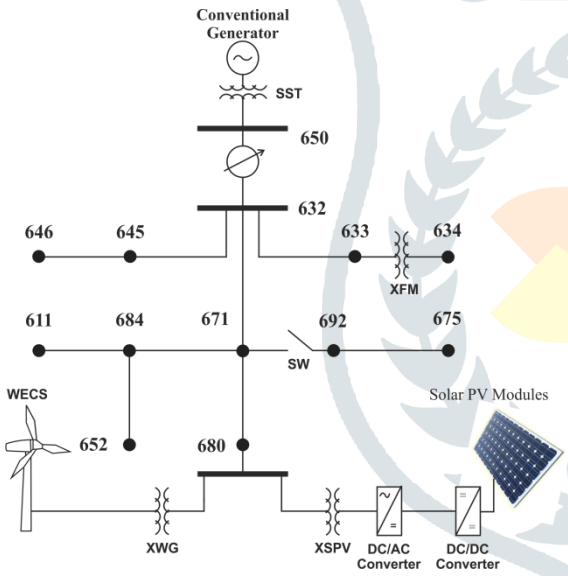

Fig. 1. Distributed generation sources based smart grid

Table 1 Loading Status of Test System Used for Smart Grid

Nodes	Load Model	Load		Capacitor banks (kVAr)
		kW	kVAr	
634	Y-PQ	400	290	
645	Y-PQ	170	125	
646	Y-PQ	230	132	
652	Y-PQ	128	86	
671	Y-PQ	1155	660	
675	Y-PQ	843	462	600
692	Y-PQ	170	151	
611	Y-PQ	170	80	100
632-671	Y-PQ	200	116	

Table 2 Transformer Data of the Test System

Transformer	MVA	kV-High	kV-Low	HV Winding		LV Winding	
				R (pu)	X pu)	R (pu)	X pu)
Substation	10	115	4.16	29.095	211.60	0.1142	0.8306
XFM	5	4.16	0.48	0.011	3.0159	0.011	3.0159
XWG	5	4.16	0.575	0.3807	2.7688	0.0510	0.0042
XSPV	5	4.16	0.260	0.001	1.1310	0.001	1.1310

The data related to wind generator, wind turbine and controllers as reported in [5] are used in the proposed study. The capacity of wind generator is 1.5 MW. The capacity of solar PV system having the capacity 1 MW is used in this study. The parameters related to solar PV array, dc-dc boost converter, inverter, filters, maximum power point tracking etc. as reported in [4] are used in this study.

3. Proposed PQ Detection Algorithm

The proposed power quality detection algorithm has been implemented with the following steps.

- The voltage signal is captured at PCC and then decomposed using S-transform to obtain S-matrix. The sampling frequency of 1.92 kHz is used and sampled over a period of 12 cycles. Stockwell transform as reported in the references [15] and [16] has been used in this study.
- The S-transform based plots such as frequency contour (S-contour), amplitude-time curve, phase curve, Absolute value curve and amplitude-frequency curve are obtained from the S-matrix. All the parameters are normalized with respect to maximum values.
- The total harmonics distortions of voltage signal (THDv) and current supplied by the DG sources at PCC (THDi) are calculated using fast Fourier transform (FFT).
- \item Power frequency variations are detected by continuous monitoring of system frequency.
- Features extracted from S-transform based plots, THDv, THDi and variations in the power frequency are processed to detect the PQ disturbances associated with various events under study.

4. Simulation Results and Discussion

This section presents the analysis of PQ events associated with various events (C1 to C6) in the DG sources based hybrid power system. The S-transform based plots of these events are compared with the respective plots of standard PQ disturbances such as voltage sag, swell, interruption, notch, spike, oscillatory transient, impulsive transient, flicker, harmonics and pure sine wave to effectively detect the PQ disturbances associated with events considered in this study. All the events have been simulated at 0.33 s.

4.1 Feeder Tripping

The tripping of feeder has been simulated at 0.33 s by opening the circuit breaker between the nodes 671-692. This feeder is supplying the inductive load as well as a capacitor bank connected on the bus 675. The various plots based on the S-transform are shown in the Fig. 2. The sharp peak available in the sum absolute values curve of Fig. 2 (d) detects the tripping of feeder as well as this is an indication of presence of PQ disturbances. An isolated contour present in the frequency contour of Fig. 2 (b) indicates the presence of oscillatory transient. The presence of OT has been validated by the finite magnitude present between the normalized frequencies 0.25 to 0.45 in Fig. 2 (f) where the finite values beyond 0.45 indicates the presence of impulsive transient. The increase in amplitude curve of the Fig. 2 (c) indicates the presence of voltage swell. The abrupt change in the phase curve of Fig. 2 (e) indicates the presence of transients. Power frequency signal with feeder tripping is shown in Fig. 3. The frequency increases to 60.1 Hz and restored to 60 Hz in 0.05 s. The values of THDv and THDi are provided in Table 3.

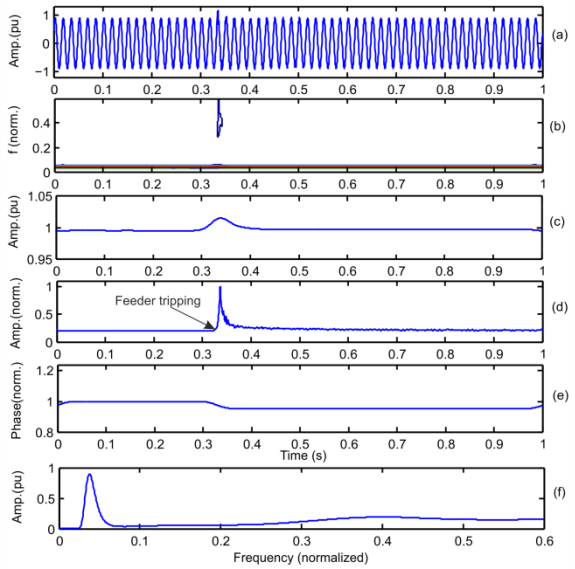

Fig. 2. (a) Voltage signal (b) frequency contour (c) amplitude curve (d) sum absolute values curve (e) phase curve (f) amplitude-frequency curve using S-transform during feeder tripping.

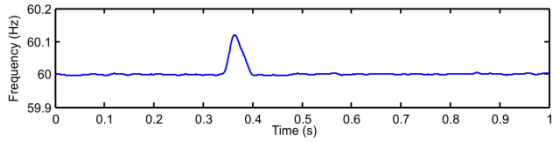

Fig. 3. Frequency variation during feeder tripping

Table 3 Total Harmonic Distortions of Voltage and Current

S.No.	Class symbol	Different cases of study	THDv (%)	THDi (%)
1	C1	Feeder tripping	0.0485	0.0382
2	C2	Feeder reclosing	0.0859	0.0792
3	C3	Switching ON the capacitor	0.0715	0.0553
4	C4	Switching OFF the capacitor	0.0558	0.0606
5	C5	Switching OFF the LR load	0.0449	0.0345
6	C6	Switching ON the LR load	0.0782	0.0859

4.2 Feeder Reclosing

The Reclosing of feeder has been simulated at 0.33 s by closing the circuit breaker between the nodes 671-692 which was initially held in open state. Various plots based on the S-transform are shown in Fig. 4. The sharp peak available in sum absolute values curve of Fig. 4 (d) detects the reclosing of feeder as well as indicates the presence of PQ disturbances. An isolated contour present in the frequency contour of Fig. 4 (b) indicates the presence of oscillatory transient. Presence of OT has also been validated by finite magnitude present between the normalized frequencies 0.15 to 0.40 in Fig. 4 (f). Decrease in magnitude of the amplitude curve of Fig. 4 (c) indicates the presence of voltage sag. The abrupt change in the phase curve of Fig. 4 (e) indicates the presence of transients in the voltage signal. Power frequency signal with tripping of the feeder is shown in Fig. 5. The frequency decreases to 59.94 Hz and restored to 60 Hz in 0.1 s. The values of THDv and THDi are provided in Table 3.

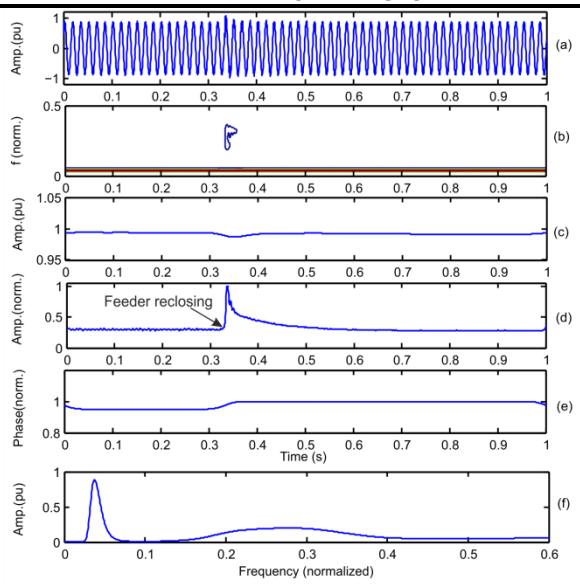

Fig. 4. (a) Voltage signal (b) frequency contour (c) amplitude curve (d) sum absolute values curve (e) phase curve (f) amplitude-frequency curve using S-transform during feeder reclosing.

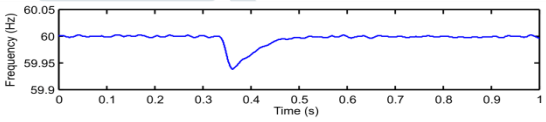

Fig. 5. Frequency variation during feeder reclosing

4.3 Switching ON the Capacitor Bank

Switching ON of the capacitor bank having the capacity of 600 kVAr om the bus 675 has been simulated at 0.33 s. This capacitor bank was initially held disconnected. The related S-transform based plots are shown in Fig. [6]. The sharp peak available in the sum absolute values curve of Fig. [6] (d) detects the event of switching on the capacitor bank. An isolated contour present in the frequency contour of Fig. [6] (b) indicates the presence of oscillatory transient. The presence of OT has also been validated by the finite magnitude present between the normalized frequencies 0.15 to 0.40 in Fig. [6] (f). Increase in the value of amplitude curve of Fig. [6] (c) indicates that the voltage increases with switching on of the capacitor bank. This has been observed due to increased level of the reactive power in the network. The abrupt change in phase curve of Fig. [6] (e) indicates the presence of low magnitude transients in the voltage signal. Power frequency signal with switching on the capacitor bank is shown in Fig. [7]. Frequency decreases to 59.98 Hz and restored to 60 Hz in 0.1 s. The values of THDv and THDi are provided in Table 3.

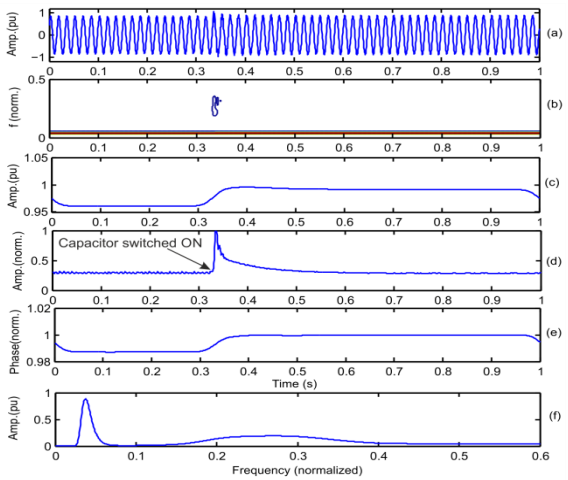

Fig. 6. (a) Voltage signal (b) frequency contour (c) amplitude curve (d) sum absolute values curve (e) phase curve (f) amplitude-frequency curve using S-transform during switching ON the capacitor bank

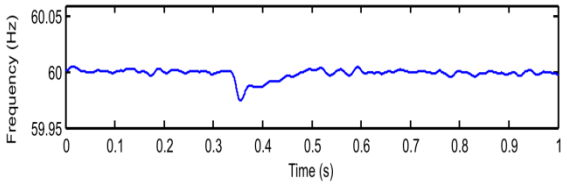

Fig. 7. Frequency variation during switching on the capacitor bank.

4.4 Switching OFF the Capacitor Bank

The capacitor having the capacity of 600 kVAr has been switched OFF at 0.33 s on bus 675. The related S-transform based plots are shown in Fig. [8]. The sharp peak available in the sum absolute values curve of Fig. [8] (d) detects the switching off the capacitor bank. A small isolated contour present in the frequency contour of Fig. [8] (b) indicates the presence of low magnitude oscillatory transient. The presence of continuous finite magnitude over the entire range of normalized frequencies in the Fig. [8] indicate the presence of impulsive transient. Decrease in the value of amplitude curve of Fig. [8] (c) indicates that the voltage decreases with switching off the capacitor bank. This is observed due to the reduced reactive power in the network. The significant change has not been observed in the phase curve of Fig. [8] (e). Power frequency signal with switching off the capacitor bank is shown in Fig. [9]. Frequency increases to 60.04 Hz and restored to 60 Hz in 0.05 s. The values of THDv and THDi are provided in the Table 3.

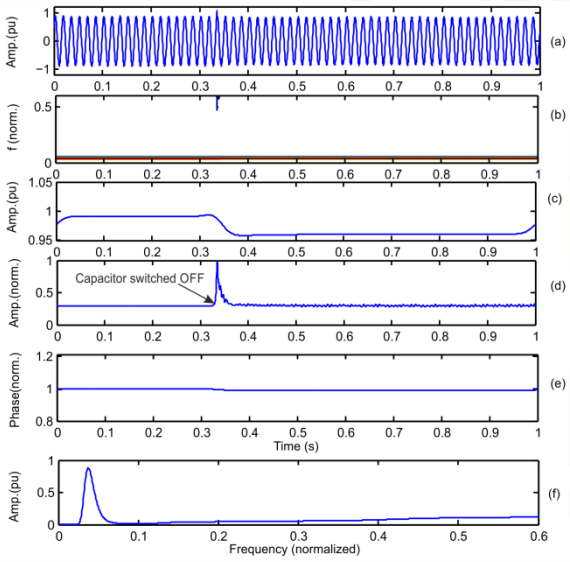

Fig. 8. (a) Voltage signal (b) frequency contour (c) amplitude curve (d) sum absolute values curve (e) phase curve (f) amplitude-frequency curve using S-transform during switching off the capacitor bank

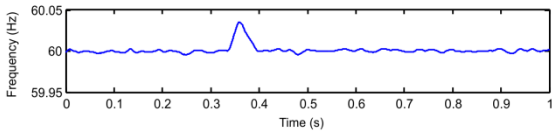

Fig. 9. Frequency variation during switching off the capacitor bank

4.5 Switching OFF the Inductive Resistive Load

The inductive resistive (LR) load on the bus 671 has been switched off at 0.33 s. The related S-transform based plots are shown in Fig. 10. The sharp peak available in the sum absolute values curve of Fig. 11 (d) detects the switching off the LR load. Isolated contour has not been observed with the frequency contour of Fig. 11 (b). Hence, oscillatory transient is not detected with the switching off the LR load. Higher frequency components are also not observed with the frequency-amplitude curve of the Fig. 11 (f). The increase in value of amplitude curve of Fig. 11 (c) indicates that the voltage increases with switching off the capacitor bank. This is observed due to the reduced demand of reactive power in the network. The significant change has also been observed in the phase curve of Fig. 11 (e). Power frequency signal with switching off the capacitor bank is shown in Fig. 12. The frequency increases to 60.18 Hz and restored to 60 Hz in 0.05 s. The values of THDv and THDi are provided in Table 3.

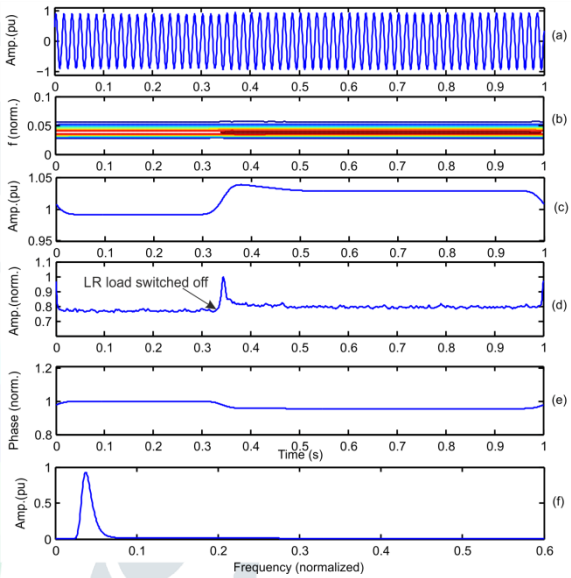

Fig. 10. (a) Voltage signal (b) frequency contour (c) amplitude curve (d) sum absolute values curve (e) phase curve (f) amplitude-frequency curve using S-transform during switching off the inductive resistive load

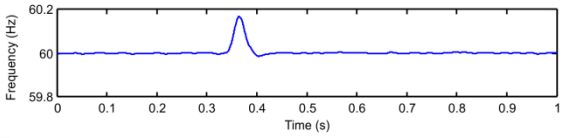

Fig. 11. Frequency variation during switching off the inductive-resistive load

4.6 Switching ON the Inductive Restive Load

The inductive resistive (LR) load on the bus 671 has been switched on at 0.33 s which was initially held disconnected. The related S-transform based plots are shown in Fig. 12. The sharp peak available in the sum absolute values curve of Fig. 12 (d) detects the switching on the LR load. Isolated contour has not been observed with the frequency contour of Fig. 12 (b). Hence, oscillatory transient is not detected with the switching on the LR load. Higher frequency components are also not observed with the frequency-amplitude curve of Fig. 12 (f). Decrease in the value of amplitude curve of Fig. 12 (c) indicates that the voltage decreases with switching off the LR load. This is observed due to the increased demand of reactive power in the network. The significant change has also been observed in the phase curve of Fig. 12 (e). Power frequency signal with switching on the LR load is shown in Fig. 13. The frequency decreases to 59.88 Hz and restored to 60 Hz in 0.05 s. The values of THDv and THDi are provided in the Table 3.

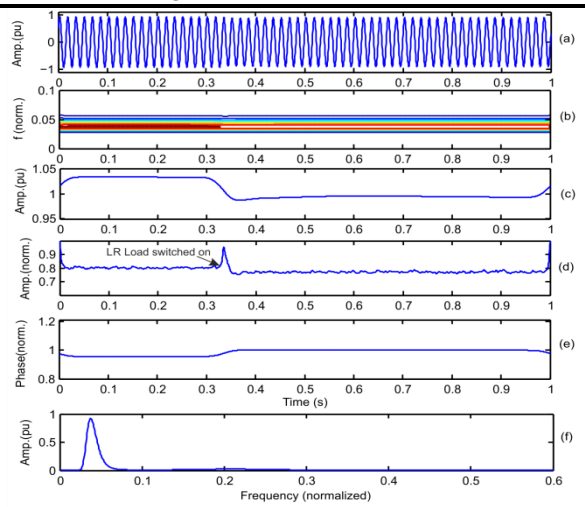

Fig. 12. (a) Voltage signal (b) frequency contour (c) amplitude curve (d) sum absolute values curve (e) phase curve (f) amplitude-frequency curve using S-transform during switching on the inductive resistive load

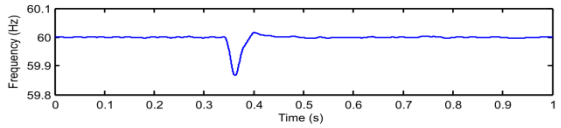

Fig. 13. Frequency variation during switching on the inductive-resistive load

The maximum deviations in the frequency are provided in the Table 4.

Table 4 Maximum Frequency Deviation with Operational Events in Smart Grid

S. No.	Case of study	Frequency deviation (Hz)
1	Feeder tripping	$11x10^4$
2	Feeder reclosing	$14x10^4$
3	Switching ON the capacitor	$5.9x10^4$
4	Switching OFF the capacitor	$5.9x10^4$
5	Switching OFF the LR load	$5.5x10^4$
6	Switching ON the LR load	$5.2x10^4$

5 Conclusion

This paper investigates the power quality disturbances in the presence of wind and solar PV systems during the events such as feeder tripping, feeder re-closing, switching on/off the capacitor bank and switching on/off the inductive resistive loads. An approach based on the S-transform has been utilized for the investigation of the PQ events associated with the various events of grid operations. The voltage signal captured at the PCC has been decomposed using S-transform and S-matrix has been obtained from which various plots known as ST plots are obtained. These plots are utilized to investigate the PQ disturbances. The power quality index has been proposed to investigate the overall effect of the events under study on the power quality. It has been concluded that OT, IT and voltage swell are associated with the feeder tripping whereas the OT and voltage sag are associated with the feeder re-closing. The oscillatory transient and voltage rise are observed with switching on the capacitor bank whereas the voltage decrease, low magnitude OT and IT are observed with the switching off the capacitor bank. Voltage rise is observed with the switching off the inductive load whereas the voltage decrease is observed with the switching on the inductive load. The harmonic distortions of voltage and current have been observed with all events of study. The power frequency variations are also observed with all events under investigation.

Reference

[1] P. K. Dash, M. Padhee, and S. K. Barik, "Estimation of power quality indices in distributed generation systems during power islanding conditions," International Journal of Electrical Power Energy Systems, vol. 36, no. 1, pp. 18 – 30, 2012.

[2] O. P. Mahela and A. G. Shaik, "Power quality improvement in distribution network using fDSTATCOMg with battery energy storage system," International Journal of Electrical Power Energy Systems, vol. 83, pp. 229 – 240, 2016.

[3] P. K. Ray, S. R. Mohanty, and N. Kishor, "Classification of power quality disturbances due to environmental characteristics in distributed generation system," IEEE Transactions on Sustainable Energy, vol. 4, no. 2, pp. 302–313, April 2013.

[4] O. P. Mahela and A. G. Shaik, "Detection of power quality events associated with grid integration of 100kw solar pv plant," in Energy Economics and Environment (ICEEE), 2015 International Conference on, March 2015, pp. 1–6.

[5] O. P. Mahela and A. G. Shaik, "Power quality detection in distribution system with wind energy penetration using discrete wavelet transform," in Advances in Computing and Communication Engineering (ICACCE), 2015 Second International Conference on, May 2015, pp. 328–333.

[6] O. P. Mahela, A. G. Shaik, and N. Gupta, "A critical review of detection and classification of power quality events," Renewable and Sustainable Energy Reviews, vol. 41, pp. 495 – 505, 2015.

[7] N. C. F. Tse, J. Y. C. Chan, W.-H. Lau, and L. L. Lai, "Hybrid wavelet and hilbert transform with frequency-shifting decomposition for power quality analysis," Instrumentation and Measurement, IEEE Transactions on, vol. 61, no. 12, pp. 3225–3233, Dec 2012.

[8] R. G. Stockwell, L. Mansinha, and R. P. Lowe, "Localization of the complex spectrum: the s-transform," Signal Processing, IEEE Transactions on, vol. 44, no. 4, pp. 998–1001, Apr 1996.

[9] H. Eristi, O. Yildirim, B. Eristi, and Y. Demir, "Automatic recognition system of underlying causes of power quality disturbances based on s-transform and extreme learning machine," International Journal of Electrical Power Energy Systems, vol. 61, pp. 553 – 562, 2014.

[10] M. Biswal and P. K. Dash, "Detection and characterization of multiple power quality disturbances with a fast s-transform and decision tree based classifier," Digital Signal Processing, vol. 23, no. 4, pp. 1071 – 1083, 2013.

[11] S. S. Kaddah, K. M. Abo-Al-Ez, T. F. Megahed, and M. G. Osman, "Probabilistic power quality indices for electric grids with increased penetration level of wind power generation," International Journal of Electrical Power Energy Systems, vol. 77, pp. 50 – 58, 2016.

[12] P. K. Ray, S. R. Mohanty, and N. Kishor, "Disturbance detection in grid-connected distributed generation system using wavelet and s-transform," Electric Power Systems Research, vol. 81, no. 3, pp. 805 – 819, 2011.

[13] C.-T. Hsu, R. Korimara, and T.-J. Cheng, "Power quality analysis for the distribution systems with a wind power generation system," Computers Electrical Engineering, pp. –, 2015.

[14] W. H. Kersting, "Radial distribution test feeders," Power Systems, IEEE Transactions on, vol. 6, no. 3, pp. 975–985, Aug 1991.

[15] P. K. Ray, N. Kishor, and S. R. Mohanty, "Islanding and power quality disturbance detection in grid-connected hybrid power system using wavelet and s -transform," Smart Grid, IEEE Transactions on, vol.3, no. 3, pp. 1082–1094, Sept 2012.

[16] B. K. Panigrahi, P. K. Dash, and J. B. V. Reddy, "Hybrid signal processing and machine intelligence techniques for detection, quantification and classification of power quality disturbances," Engineering Applications of Artificial Intelligence, vol. 22, no. 3, pp. 442 – 454, 2009.